Electromechanical actuation of macroscopic carbon nanotube structures: mats and aligned ribbons

Daniela Suppiger,[a] Stephan Busato,*[a] Paolo Ermanni,[a] Marcelo Motta[b] and Alan Windle[b]

Received 19th December 2008, Accepted 12th March 2009
First published as an Advance Article on the web 9th April 2009
DOI: 10.1039/b822862k

The electromechanical actuation of macroscopic carbon nanotube (CNT) structures, including single and multi walled CNT mats and aligned ribbons, is analyzed and compared. From experimental evidence, actuation due to quantum chemical and electrostatic effects can be distinguished. Their respective contribution to the total actuation depends on two key parameters, namely Young's modulus and charge density. While mechanical energy densities of actuated structures are appreciable, electromechanical conversion efficiencies are found to be impractically low.

1. Introduction

Due to their unique combination of properties, carbon nanotubes (CNTs) have attracted a great deal of interest for use as electromechanical actuators.[1] Individual carbon nanotubes combine excellent electrical and thermal conductivities with remarkable mechanical properties, currently being the strongest and stiffest materials known. However, these properties are still to be realized when the tubes are assembled into a useful macroscopic form. A practical approach to manufacture a manageable structure of carbon nanotubes is their assembly into buckypapers. Buckypapers are sheets of highly entangled single or multi-walled nanotubes (SWCNTs or MWCNTs) held together by van der Waals interactions. These structures provide sufficient mechanical properties to permit their evaluation as actuators.

The concept of using SWCNT buckypapers as electromechanical actuators was introduced some ten years ago.[2] The authors observed a quasi-parabolic relationship between the applied potential and the strain generated in the in-plane direction. This actuation was attributed to dimensional changes of the covalent bond network along the nanotube direction as a consequence of quantum chemical effects arising from charge injection into the tubes. From experimental data obtained on a SWCNT buckypaper, the maximum actuation strain for nanotube sheets composed of isolated (nonbundled) SWCNTs was predicted to be around 1–1.2% for operation in aqueous electrolytes with a 1 V operation range. Actuation is not limited to SWCNTs, but was also observed in MWCNT buckypapers.[3]

It has been pointed out,[4] that the realization of the full potential of SWCNTs as actuators will depend on a significant improvement of the ability of macroscopic CNT structures to generate stress at levels required in most practical applications. Mechanical properties of typically used SWCNT buckypapers are orders of magnitude lower than the values for individual nanotubes, and actually measured in-plane actuation strains amount to *ca.* 0.04%.[5] While much stiffer macroscopic CNT structures have been reported, no corresponding actuation data are available. Essentially, a CNT actuator with a modulus in the terapascal range and an active strain of 1% is not in sight.

One approach for increasing the mechanical properties of macroscopic CNT structures has been found in the direct-spinning of a CNT aerogel,[6] yielding aligned ribbons composed purely of CNTs, with strengths and stiffnesses from one to two orders of magnitude higher than buckypapers, and ultimate tensile strains of 5–10%. These improved properties arise from the high contact area between the individual tubes as well as the high degree of internal alignment.[7]

As part of our ongoing investigations into manufacturing robust and reliable active devices consisting of carbon nanotubes, here we report on actuation experiments performed on single walled carbon nanotube buckypapers, multi walled carbon nanotube buckypapers and aligned carbon nanotube ribbons. These structures allow comparison of actuation over a rather wide range of Young's moduli. In particular, the interrelationship between actuation strain and material properties such as electrical charge storage capability (electrical capacitance) and mechanical properties is assessed.

2. Experimental

Two commercially available grades of SWCNTs were used (HeJi Inc., China, 95% nominal purity, mean od 1–2 nm, length 10–20 μm; Nanoledge, France, 60% purity) and one grade of MWCNTs (Bayer Material Science, Germany, Baytubes C 150 P, 95% purity, mean od 13–16 nm, length 1–10 μm, number of walls 3–15). Experimental details of buckypaper manufacturing have been described elsewhere.[8] In the manufacturing process of the SWCNTs buckypapers, centrifuged and uncentrifuged dispersions were used, whereas for MWCNTs only centrifuged dispersions were used. Centrifugation typically leads to buckypapers of

[a] *Centre of Structure Technologies, ETH Zurich, Leonhardstrasse 27, 8092, Zürich, Switzerland*
[b] *Department of Materials Science & Metallurgy, University of Cambridge, Pembroke Street, Cambridge, UK CB2 3QZ*

higher modulus. Buckypapers are stated as He-c (HeJi centrifuged), He-uc (HeJi uncentrifuged), and Na-uc (Nanoledge uncentrifuged) and Bay-c (Baytubes centrifuged). The Nanoledge centrifuged buckypaper did not yield a cohesive mat.

Aligned carbon nanotube ribbons were produced by the direct-spinning process developed at the university of Cambridge,[6] where an aerogel composed of carbon nanotubes is continuously spun directly from the hot zone of a chemical vapor deposition reactor. The ribbons are composed of mainly double-walled tubes with minimum presence of impurities, typically up to 5 wt% residual catalyst particles (Fe) and a small amount of amorphous carbon coating. Moreover, they are predominantly oriented along the ribbon axis.[7]

While theoretical work[9] does examine the different actuation behavior of the various CNT flavors, for obvious practical reasons the CNT structures investigated here consisted of available materials of not fully determined composition. It was beyond the scope of this work to fully characterize the materials other than to check for impurities following reported procedures.[8]

The morphologies of buckypaper and aligned ribbon surfaces were examined with a Scanning Electron Microscope (SEM) Gemini LEO 1530. Transmission Electron Microscope (TEM) analyses of aligned ribbons were performed on a cold field emission TECNAI F20 operated at 200 kV. The specific surface area was characterized by the Brunauer–Emmett–Teller (BET) method using a TriStar Micromeritics analyzer. Prior to measurements, samples were preconditioned under nitrogen for 1 h at 150 °C using a Flow Prep 060 Micromeritics. Mechanical properties of the different CNT materials in the dry state were determined from tensile tests on an Instron 5864 tensile tester at a strain rate of 10% min^{-1}. The specific electric double layer capacitance C_g [F g^{-1}] of samples immersed in 1 M NaCl was determined under galvanostatic conditions using the equation $C_g = (I\Delta t)/(m\Delta U)$, where I [A] is the applied current, Δt [s] the time required for a potential change ΔU [V] and m [g] the mass of the buckypaper.[10]

The in-plane (longitudinal) actuation strain in 1 M NaCl was measured using a dynamic mechanical analyzer (Perkin Elmer DMA 7e) in static tensile mode (Fig. 1). Buckypaper strips and aligned ribbons were clamped to have an active length of 6–7 mm and immersed in the liquid electrolyte. Nearly free-strain conditions were set up by applying a minimal tensile load of 10 mN required for stable tensile strain measurements. A buckypaper of similar size was used as counter electrode and a saturated calomel electrode (SCE) as reference electrode. Voltage steps (positive and negative potentials) of 1 min duration were applied by the potentiostat and the measured displacement used to determine actuation strain. Reported strain values represent mean values of measurements on three to ten specimens for each CNT structure; reproducibility was better than 5%.

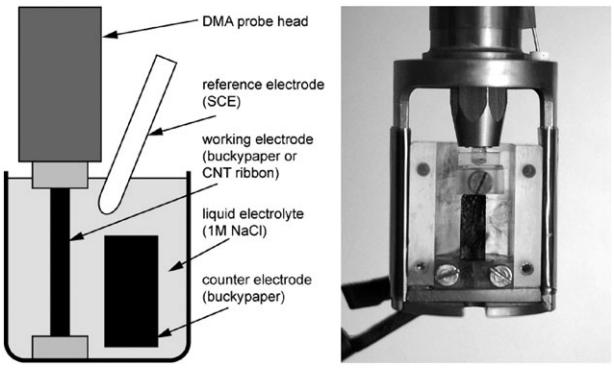

Fig. 1 Schematic (left) and photograph (right) of experimental setup for in-plane actuation strain measurements.

3. Results and discussion

SEM images reveal the morphology of the single and multi-walled CNT buckypapers (Fig. 2a–d) as well as the aligned ribbons (Fig. 2e). All samples display a distinctly fibrillar structure, with the exception of Na-uc buckypaper (Fig. 2c), possessing particulate features attributed to the elevated amorphous carbon content. The TEM image of aligned ribbons (Fig. 2f) shows that the tubes making up the ribbon are double walled. An analysis of fibril diameters suggests that the SWCNT buckypapers, He-c and He-uc (Fig. 2a and b), consist of bundles (diameter 10–25 nm) of agglomerated rather than individual tubes (diameter 1–2 nm). MWCNT buckypaper Bay-c (Fig. 2d) also consists of bundles (20–30 nm), with a diameter closer to individual tubes (13–16 nm) indicating a lower degree of agglomeration. Finally, fibril diameters in the aligned ribbons (Fig. 2e) range from 5 to 20 nm, implying the presence of individual tubes (5 nm).

In the potential range of −0.8 to +1.1 V *vs.* SCE, representing the conservative electrochemical stability window of 1 M

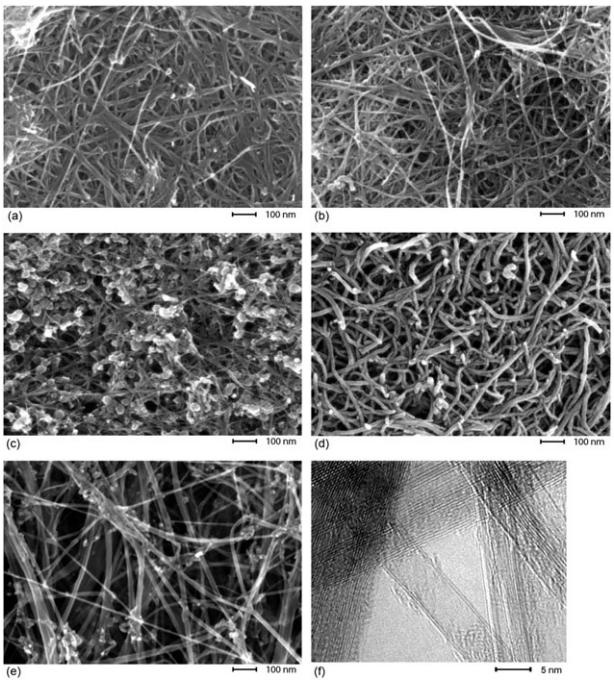

Fig. 2 SEM images: (a) SWCNT He-c buckypaper; (b) SWCNT He-uc buckypaper; (c) SWCNT Na-uc buckypaper; (d) MWCNT Bay-c buckypaper; (e) aligned ribbons and (f) TEM image of aligned ribbons.

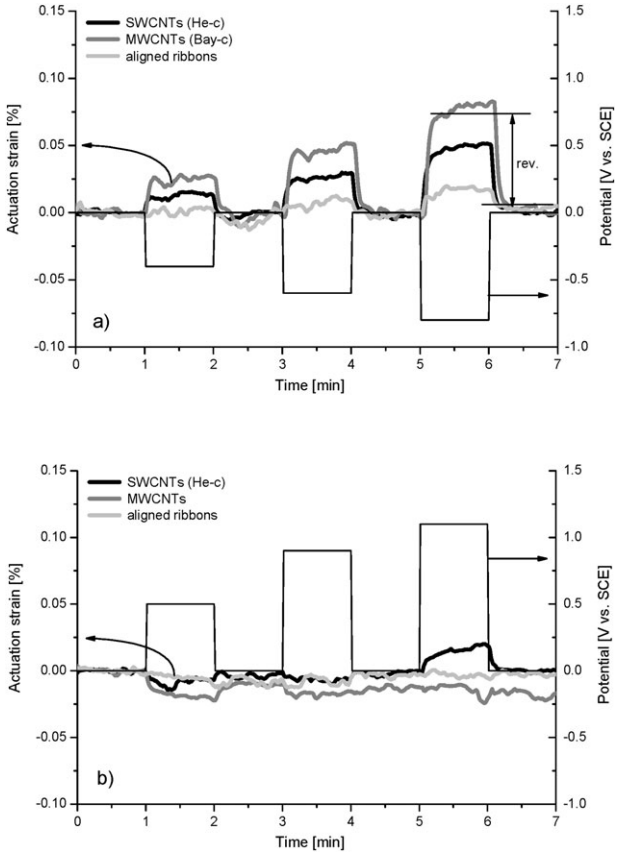

Fig. 3 Actuation of macroscopic CNT structures in 1 M NaCl at negative (a) and positive (b) potentials: comparison of SWCNT buckypaper (He-c), MWCNT buckypaper (Bay-c) and aligned ribbons. For reasons of clarity Na-c and He-uc materials are omitted in this figure; however data of all samples are shown in the following figures.

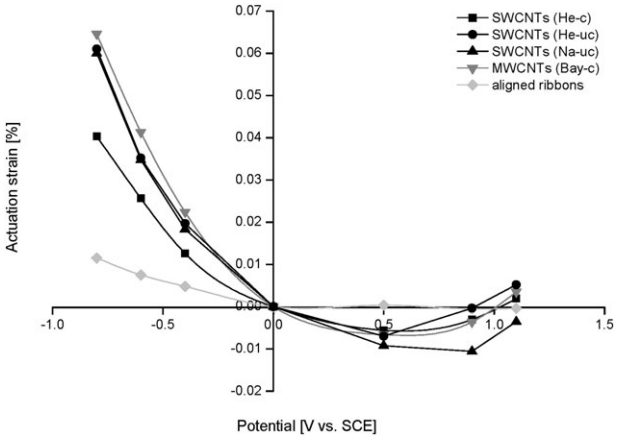

Fig. 4 Reversible free actuation strain (zero tensile prestress) of SWCNT/MWCNT buckypapers and aligned ribbons in 1 M NaCl. The lines do not represent fits, but serve to guide the eye.

NaCl, all structures examined display a reversible actuation, irrespective of the underlying CNT type. Observed actuation strains are significant for negative potentials only (Fig. 3a) and negligible for positive potentials (Fig. 3b).

The free reversible actuation strain is determined as the difference between the average strain during an actuation period and the subsequent period at zero potential (Fig. 4). Maximum actuation strain is observed at −0.8 V for all samples, being lowest for the stiff aligned ribbons and largest for MWCNTs Bay-c. All samples show lowest extension not at zero potential, but at +0.5 to +0.9 V, except for the aligned ribbons, where no actuation at all is detected at positive potentials.

Table 1 summarizes physical properties as measured on the different CNT structures.

Young's moduli vary over a range of nearly two orders of magnitude, reflecting the different entanglement densities and degrees of CNT overlap in the various structures. A clear correlation can be seen between BET surface and specific electrical capacitance, as one would expect for materials behaving as electric double-layer capacitors.

On the other hand, maximum observed actuation (at −0.8 V) does not correlate with specific capacitance (Fig. 5): An actuation strain of *ca.* 0.06% is observed for both MWCNT Bay-c and SWCNT He-uc, two samples differing in specific capacitance by a factor of three (17.5 and 40 F g^{-1}, respectively). At the same time aligned ribbons of somewhat lower capacitance (11.2 F g^{-1}) display an active strain five times lower than the MWCNT Bay-c sample (0.012 and 0.064%, respectively). Fig. 5 connotes that specific capacitance is not the primary parameter affecting actuation strain of the materials examined.

When analyzing actuation strain as a function of modulus, however, a much stronger correlation is apparent (Fig. 6): the higher the modulus the lower the strain. Highest strain is found in the most compliant CNT structure (MWCNT Bay-c), whereas the stiffest structure exhibits the lowest strain (aligned ribbons). In the semilogarithmic plot of Fig. 6, the remaining samples of intermediate modulus appear to be situated on a straight line between the two extremes. Most notable in this respect are the actuation behaviors of SWCNT buckypapers He-uc and He-c, both constituted of the identical raw material and possessing similar specific capacitance, but significantly different moduli: the more compliant He-uc features the higher strain. From the virtually common intercepts of the three linear fit curves with the *x*-axis in Fig. 6, one might be led to infer a modulus-of-zero-actuation for a CNT structure at 40–50 GPa, independent of the underlying CNT type. Moduli of buckypapers in the wetted state during actuation experiments are typically lower than those measured in the dry state.[11] This has to be taken into account when assessing Fig. 6.

At first glance, these findings are not concordant with the ideas put forward in ref. 2. Actuation of SWCNT buckypapers was attributed to an effect known to occur in graphite intercalation compounds (GIC), namely a change in the lattice constant of the graphene atomic lattice with charge injection into the graphene pi-orbital system. This quantum chemical effect was deemed greater than classical coulombic effects for the actuation of carbon nanotube sheets. Such an actuation mechanism implies an actuation strain dependent mainly on the electrical charge on the nanotubes (*i.e.* specific capacitance), but independent of the mechanical properties of the macroscopic structure. Our findings (Fig. 5 and Fig. 6) show quite the opposite.

Table 1 Physical properties of SWCNT buckypapers, MWCNT buckypapers and aligned ribbons

Property	Measurement units	SWCNTs BP He-c	SWCNTs BP He-uc	SWCNTs BP Na-uc	MWCNTs BP Bay-c	Aligned ribbon
Density (bulk)	g cm^{-3}	0.64	0.29	0.48	0.45	0.8
Young's modulus	MPa	2509	758	429	335	16000
Stress at break	MPa	18	5	4	3	1000
Strain at break	%	2.1	1.5	1.8	2	5
Specific surface area	m^2 g^{-1}	510	535	154	174	165
Specific electrical capacitance	F g^{-1}	35	40	19	17.5	11.2

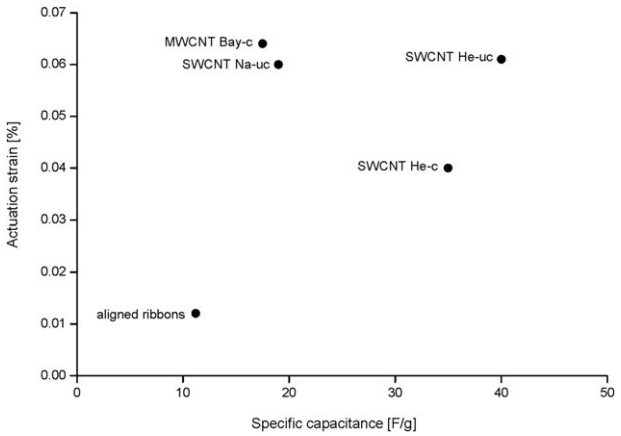

Fig. 5 Actuation strain at −0.8 V *vs.* SCE as a function of specific capacitance (both in 1 M NaCl).

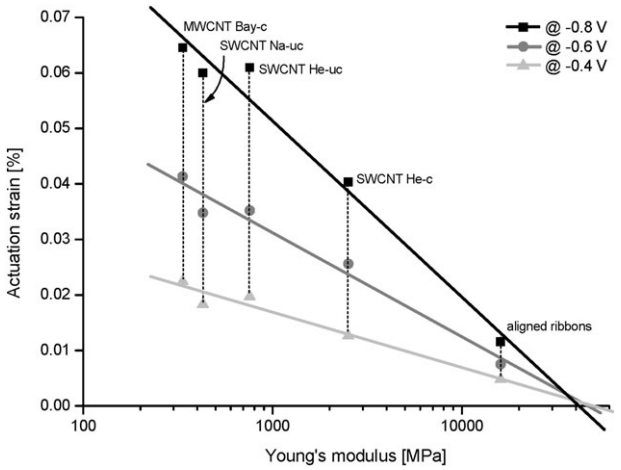

Fig. 6 Actuation strain in 1 M NaCl at different potentials *vs.* Young's modulus in dry state.

The discrepancy between suggested mechanism and experimental observation becomes more explicit, when analyzing strain as a function of nominal charge density. For each experimental strain *vs.* potential value in Fig. 4, the corresponding nominal charge per 100 carbon atoms value is derived using the equation $Q_C = 100(C_g U 1/n)/(1/12N_A)$, where Q_C is the nominal charge per 100 carbon atoms expressed in number of electron charges [e^-], C_g the specific capacitance [F g^{-1}], U the potential [V *vs.* SCE], n the charge of an electron [1.6 × 10^{-19} C] and N_A the Avogadro constant

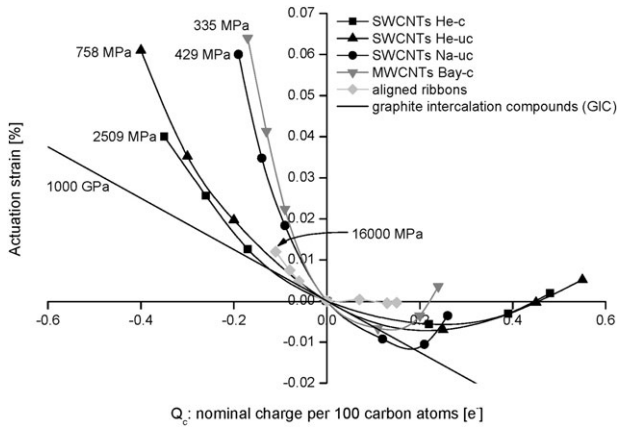

Fig. 7 Actuation strain *vs.* nominal charge density Q_c. Elastic moduli in the dry state are given next to curves for each structure; for graphite intercalation compounds the value of graphene is given.[13]

[6.02 × 10^{23} mol^{-1}]. Calculation of nominal charge is thus based on the measured specific capacitance and the simplifying assumption that all carbon atoms, including those of inner MWCNT walls and of carbonaceous impurities, are equally charged. However, the true percentage of charge actually transferred to the carbon atoms and the true charge distribution are unknown, a caveat to be considered in the interpretation. Included in Fig. 7 is a straight line representing a linear fit to the collection of data for graphite intercalation compounds presented in ref. 12.

Buckypapers on one-hand and aligned ribbons on the other show slightly different strain *vs.* charge density characteristics:

For negatively charged buckypapers of low nominal charge density Q_C, the strain produced for a given amount of charge is considerably higher for the more compliant structures. With increasing modulus actuation strain is reduced and approaches the values found in GICs. With increasingly negative charge densities, actuation for all structures digresses to significantly higher strains than found in GICs. The interpretation is, that for buckypapers of high modulus and at low values of Q_C (less than −0.1 e^-/100 carbon atoms), quantum chemical effects as observed in GICs may well determine actuation behavior. However, actuation of structures of low modulus and/or at high charge densities is clearly dominated by other effects. The most likely cause in those cases is electrostatic repulsion between individual, electrically charged nanotubes or bundles making up the structure. This interpretation is substantiated by the near-parabolic shape of the curves in Fig. 7.

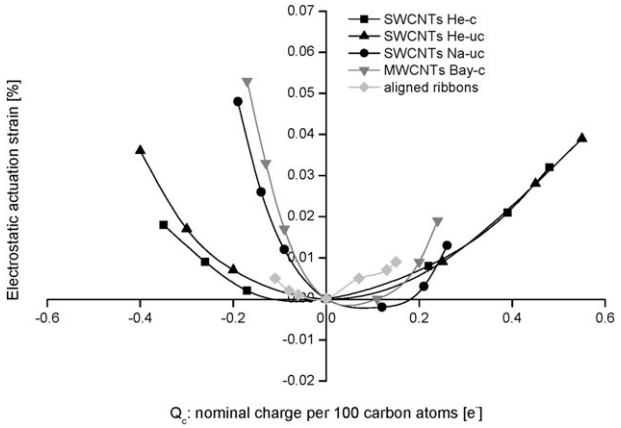

Fig. 8 Contribution of electrostatic effects to the overall actuation. For details see text.

For positive nominal charges, the strains generated by quantum chemical and electrostatic effects are no longer of the same sign, but opposing each other. Positively charged buckypapers at low charge densities all show the negative strain (contraction) as seen in GICs, further corroborating quantum chemical C–C bond shortening as the mechanism for actuation. Differences between the various buckypapers become only apparent at higher charge densities Q_C (more than 0.1 e^-/100 carbon atoms). Parabolic behavior is seen again, with the electrostatic effects described above becoming dominant and having a bigger impact on low modulus structures, expanding them more easily than stiff ones.

The superposition of quantum chemical and electrostatic effects becomes visually more evident, when subtracting the GIC line in Fig. 7 from the experimental curves. The results are near-parabolic curves, representing the contribution of electrostatic effects to the total actuation (Fig. 8). A more differentiated analysis would take into account the specific type of CNTs that actually compose the structures, and use the corresponding charge strain characteristics, instead of the generic GIC line. However, these characteristics are not overly different,[9] and since the composition is not known in such details, the application of the GIC line is deemed acceptable in the present context. Quite noteworthy is the fact that the minimum strains for MWCNT Bay-c and SWCNT Na-uc lie at positive values of Q_C, implying a point-of-zero-charge (pzc) at positive potentials *vs.* SCE. For the other samples, the minimum is located at or just below $Q_C = 0$. It is well known[14] that the pzc of graphite in aqueous electrolytes is more negative (*ca.* −0.2 V *vs.* SCE) than that of activated carbon (*ca.* 0.15 V *vs.* SCE). This is related to differences in surface polarization arising from oxidized surface groups on edge planes in activated carbon, which in turn shift the pzc to more positive values. By contrast, the basal planes of graphite are chemically much less reactive and not as easily oxidized. Both SWCNT Na-uc (nominal purity 60%) as well as MWCNT Bay-c apparently contain more oxidized species than the other samples.

Aligned ribbons exhibit no actuation strain at positive charge densities. Their gravimetrical density is the highest of all structures examined (Table 1) as a corollary to enhanced nanotube overlap and reduced intertube distance responsible for their elevated mechanical properties. It is assumed that the low intertube distance increases electrostatic repulsion to the point of effectively counteracting quantum chemical contraction even at low positive values of Q_C, resulting in a net zero actuation. In theoretical considerations of SWCNT actuation,[9] the calculated charge–strain characteristics strongly depended on the choice of the value for the intertube distance.

Charge densities on all the CNT structures examined in this work are much lower than what is required for a 1% expansion of the C–C bond length (*ca.* 16 e^-/100 carbon atoms at negative charge) in a graphite intercalation compound. From experimental data, the double layer capacitance of an isolated SWCNT has been estimated at 160 F g^{-1},[2] double the value obtained from a theoretical estimation (0.01 e^-/carbon atom/V).[15] At a potential of −1.0 V this corresponds to a charge density Q_C of −1.99 e^-/100 carbon atoms and an actuation strain of 0.12%, assuming the linear GIC curve in Fig. 7 to be applicable to SWCNTs. This strain is only twice the highest strains observed in the buckypapers of this work at a fraction of the charge density.

One measure of the effectiveness, with which an electromechanical material converts electrical input energy into useful mechanical energy is the coupling coefficient k. k^2 is defined as the gravimetric ratio of converted mechanical energy E_m ($=1/2 \times$ modulus $\times$ strain^2) to electrical input energy E_e ($=1/2C_gU^2$). All structures examined in this work yielded k^2-values below 0.004% at −0.8 V, making them highly inefficient electromechanical actuators. Measured actuation strains (Fig. 4), combined with mechanical energy densities of 0.1–0.5 J kg^{-1}, put them on a par with piezoelectric polymers.[16] However, when taking into account the effectively lower modulus of buckypapers in the wet state,[11] values for k^2 and mechanical energy densities reported here are upper bounds. The isolated SWCNT described above, strained to 0.12% at −1.0 V, would yield a k^2 value of 0.67% (assuming a modulus of 1 TPa and a density of 1.35 g cm^{-3}), still an insignificant value. At the same time, the mechanical energy density would amount to 541 J kg^{-1}, exceeding most other actuator materials,[16] and the electrical energy density would amount to 80 J g^{-1} or 288 W h kg^{-1}, exceeding the value of lithium ion batteries.

To realize the ideal macroscopic CNT structure with the same mechanical properties as an individual SWCNT is still an unresolved task at present, despite considerable progress as evidenced in the aligned ribbons used in this work. To realize such a structure without giving away the high specific surface area and specific capacitance of an individual SWCNT remains a challenge even at the conceptional level. Finally, from evidence presented here it can be concluded, that even the ideal macroscopic CNT structure would not exceed the active strain seen in graphite intercalation compounds, *i.e.* 0.12% at −1 V for operation in aqueous (non-intercalating[4]) electrolytes. In combination with the very low electromechanical conversion efficiency and the very high mechanical and electric energy densities, such an actuator would find use for a limited range of applications only. A corresponding active system would have to be able to store and shuttle a large amount of "dead" electrical energy.

4. Conclusion

Electromechanical actuation of macroscopic carbon nanotube structures is experimentally found to result from a superposition of quantum chemical effects within individual nanotubes, and electrostatic effects between separate nanotubes or bundles. The former are only of significance at low charge densities (up to ± 0.1 e^-/100 carbon atoms), while for higher densities electrostatic repulsion between the constituents of the structure dominates actuation behavior.

With increasing elastic modulus of the structure, observed actuation strain approaches the linear strain *vs.* charge characteristics observed in graphite intercalation compounds (GIC). This leads to the conclusion that any structure based on graphene type constituents will fundamentally exhibit these same characteristics. If the structure's modulus is lower than that of graphene, additional electrostatic repulsion will result in an actuation strain larger than that observed in GICs.

Finally, for the aqueous, non-faradaic CNT actuators examined, mechanical output energies are comparable to those of piezoelectric polymers, albeit at very low electromechanical conversion efficiencies. Tangible improvements in actuator performance are to be expected when increasing the mechanical properties of macroscopic CNT structures and at the same time elevating charge density to a level not attainable with electric double layer charging.

Acknowledgements

We would like to thank Björn Schimmöller (Particle Technology, ETH Zurich) for BET measurements and Peter Wägli (Electron Microscopy Centre, ETH Zurich) for the SEM images and the Swiss National Science Foundation (SNF) for the financial support.

References

1 C. Li, E. T. Thostenson and T.-W. Chou, *Composites Science and Technology*, 2008, **68**, 1227–1249.
2 R. H. Baughman, C. Cui, A. A. Zakhidov, Z. Iqbal, J. N. Barisci, G. M. Spinks, G. G. Wallace, A. Mazzoldi, D. De Rossi, A. G. Rinzler, O. Jaschinski, S. Roth and M. Kertesz, *Science*, 1999, **284**, 1340–1344.
3 M. Hughes and G. Spinks, *Adv. Mater.*, 2005, **17**, 443–446.
4 S. Gupta, *Diamond Relat. Mater.*, 2006, **15**, 378–384.
5 J. Fraysse, A. I. Minett, O. Jaschinski, G. S. Duesberg and S. Roth, *Carbon*, 2002, **40**, 1735–1739.
6 M. Motta, Y. L. Li, I. Kinloch and A. Windle, *Nano Lett.*, 2005, **5**, 1529–1533.
7 M. Motta, A. Moisala, I. A. Kinloch and A. H. Windle, *Adv. Mater.*, 2007, **19**, 3721–3726.
8 D. Suppiger, S. Busato and P. Ermanni, *Carbon*, 2008, **46**, 1085–1090.
9 G. Sun, J. Kurti, M. Kertesz and R. Baughman, *J. Am. Chem. Soc.*, 2002, **124**, 15076–15080.
10 S. Shiraishi, H. Kurihara and A. Oya, *Electrochemistry*, 2001, **69**, 440–443.
11 P. G. Whitten, G. M. Spinks and G. G. Wallace, *Carbon*, 2005, **43**, 1891–1896.
12 S. Roth and R. H. Baughman, *Curr. Appl. Phys.*, 2002, **2**, 311–314.
13 C. D. Reddy, S. Rajendran and K. M. Liew, *Nanotechnology*, 2006, **17**, 864–870.
14 D. Golub, A. Soffer and Y. Oren, *J. Electroanal. Chem.*, 1989, **260**, 383–392.
15 J. A. Sippel-Oakley, PhD Thesis, University of Florida, 2005.
16 J. E. Huber, N. A. Fleck and M. F. Ashby, *Proc. R. Soc. A: Math. Phys. Eng. Sci.*, 1997, **453**, 2185–2205.